Field Crops Research 277 (2022) 108407

Contents lists available at ScienceDirect

Field Crops Research

journal homepage: www.elsevier.com/locate/fcr

Estimating early season growth and biomass of field pea for selection of divergent ideotypes using proximal sensing

Abeya Temesgen Tefera [a,*], Bikram Pratap Banerjee [a], Babu Ram Pandey [a], Laura James [b], Ramesh Raj Puri [a], Onella Cooray [a], Jasmine Marsh [a], Mark Richards [c], Surya Kant [a], Glenn J. Fitzgerald [a], Garry Mark Rosewarne [a]

[a] Agriculture Victoria Research, Horsham, VIC 3400, Australia
[b] School of Natural Sciences, University of Tasmania, Private Bag 55, Hobart, TAS, Australia
[c] NSW Department of Primary Industries, Wagga Wagga Agricultural Institute, Pine Gully Road, Wagga Wagga, NSW 2650, Australia

ARTICLE INFO

Keywords:
Crop circle
Field pea
NDVI
UAV
Vegetation indices

ABSTRACT

The aims of this study were to (i) test ground and aerial-based remote sensing vegetation indices (VIs) for trait-based breeding line selection, (ii) improve our understanding of the association between measured plant traits and readings derived from active and passive sensors and (iii) establish an optimal time for growth assessments in relation to field pea vigour and seed yield. Multispectral sensors were deployed with the handheld Crop Circle (CC) and a sensor mounted on an unmanned aerial vehicle (UAV) to collect data from field trials conducted between 2017 and 2020 at Beulah and Horsham in Victoria and Yenda, Wagga Wagga and Ardlethan in New South Wales in Australia. The result showed that normalised difference vegetation index (NDVI) derived from an aerial-based passive sensor (UAV) was strongly and significantly correlated to NDVI derived from a ground-based active sensor (CC) at both Beulah ($R^2 = 0.85$; $n = 1165$; $p < 0.001$) and Horsham ($R^2 = 0.77$; $n = 210$; $p < 0.001$). Both methods showed similar NDVI trends in pea genotype rankings. Based on the three seasons of field trial data, NDVI derived from both the CC and UAV sensors were linearly related to biomass production during pre-canopy closure growth. In water limiting environments, seed yield was positively correlated to NDVI measures. Measures calculated from the area under the NDVI curve throughout the growth season, and an additive main effect and multiplicative interaction model (AMMI) identified varieties with high vigour scores (high NDVI). Overall, a high vigour score was correlated to seed yield in lower yielding environments. From these results it appeared that higher vigour helps achieve higher yields in drier environments, however it was correlated with lower yields in better environments.

1. Introduction

Field-based phenotyping of plant traits is a routine breeding activity in field pea improvement. However, physical measurements of several quantitative traits are destructive, time-consuming, labour-intensive and expensive. Plant phenotyping using ground-based sensors and remote sensors mounted on unmanned aerial vehicles (UAVs) could provide field pea breeders with a rapid and efficient tool for trait-based phenotypic selection and help define the relationship between vigour and yield. Several studies have shown the advantages of aerial-based passive sensors over ground based active sensors in providing a wide range of vegetation indices for large-scale rapid assessment of crop growth (Winterhalter et al., 2013, 2012; Hatfield, 2008). Despite these advantages, the data quality of aerial-based passive sensors can be affected by bad weather conditions (Erdle et al., 2011; Stamatis et al., 2009; Hatfield et al., 2008) and breeders require base level information on which indices are most appropriate to facilitate the correct choice of sensors for trait-based germplasm screening.

High-throughput phenotyping through a range of spectral reflectance indices has been widely used in cereal crops for the screening of desirable plant traits adapted to abiotic and biotic stresses, including drought (Condorelli et al., 2018; Gupta et al., 2012; Kim et al., 2020), nutrition (Tan et al., 2020), frost (Nuttall et al., 2019), salinity (Beisel et al., 2018), heat (Ullah et al., 2019), herbicide, weed infestation (Huang et al., 2018), insect pest infestation (Bhattarai et al., 2019) and disease incidence (Su et al., 2018). Such indices have been used to screen

* Corresponding author.
E-mail address: abeya.tefera@ecodev.vic.gov.au (A.T. Tefera).

https://doi.org/10.1016/j.fcr.2021.108407
Received 18 June 2021; Received in revised form 20 November 2021; Accepted 16 December 2021
Available online 21 December 2021

germplasm for genetic variability, thereby increasing breeding efficiencies in field crops (Li et al., 2014). The commonly used vegetation indices, such as normalized difference vegetation index (NDVI), have the potential to be linked to important production traits, including biomass, leaf expansion, vigorous growth, yield and yield related traits in field pea.

Vegetation indices quantify plant traits based on photosynthetic activity (chlorophyll or greenness) (Beck et al., 2006; Gitelson et al., 2003,1993, 1994). It is likely that plant shoot architecture such as leaf angle, leaf orientation, leaf morphology and branching could impact the measurements derived from vegetation indices. For example, a significant correlation was reported between leaf angle and digital ground cover (DGC) in four large wheat populations (Mullan and Reynolds, 2010). However, the quantification primarily depends on chlorophyll pigments which absorb the red spectral band and reflection of near infra-red (NIR) band from the canopy. Therefore, high NDVI values are a function of low reflectance in the red spectral region and high reflectance in the infrared spectrum. NDVI and other related indices can be used to track early growth and vigour, traits which are important in crops that suffer from limited water availability due to rainfall variability and poor soil water holding capacity.

Early vigour has been proposed for drought adaptation and this is particularly relevant to field pea as the crop is seen as the preferred pulse in the drier cropping regions of south western and south eastern Australia. Inadequate water is often the main constraint affecting dry matter biomass production and seed yield in these regions. Soil water losses in this environment are mainly driven by high temperature and high atmospheric vapour pressure deficit as the season progresses (French, 2010). Leuning et al. (1994) reported soil water loss of 49% below wheat canopies in relation to total seasonal evapotranspiration in drier, Mediterranean type environments. Here, early vigour is an important plant trait in reducing water loss from the soil surface through increased ground cover and early crop development. Mullan and Reynolds (2010) found significant and negative correlations between DGC and daily soil evaporation below the wheat crop canopy. In agreement with this study, a low evaporation rate was reported under higher vigour breeding lines of wheat in water-limiting environments (Turner and Nicolas, 1998).

Early vigour is characterized by fast leaf area expansion and aboveground biomass production during the early stage of plant growth. Several studies reported positive correlations between early vigour as measured by biomass and leaf traits, such as leaf width, leaf size and specific leaf area in wheat and rice crops (Maydup et al., 2012; Rebolledo et al., 2012; Mir-Mahmoodi and Soleimanzadeh, 2009). Nguyen et al. (2018) also found strong and significant correlations between early vigour (as measured by digital ground cover, DGC) and aboveground biomass ($r = 0.92$; $p < 0.001$), leaf area ($r = 0.95$: $p < 0.001$) and water use efficiency ($r = 0.80$; $p < 0.001$ under controlled environments in field pea. These traits could be important in improving seed yield of field pea through rapid early ground cover and increasing transpiration efficiency (Ward et al., 2007) in water-limiting environments.

During early growth of wheat, Mullan and Reynolds (2010) also reported significant and positive correlations between DGC and destructive early vigour measurements, viz., biomass ($r^2 = 0.63$) and leaf area index ($r^2 = 0.84$). Their study further indicated a significant and positive correlation between DGC and NDVI ($r^2 = 0.69$) derived from GreenSeeker. Nguyen et al. (2018) also found a significant and positive correlation between DGC and NDVI derived from CC ($r = 0.70$; $p < 0.001$), indicating that NDVI is an alternative method of measuring DGC or early vigour in field pea.

The non-destructive measurement of early vigour, and potentially other plant traits, could have a significant contribution to a field pea breeding program where thousands of breeding lines are evaluated during the selection process in early breeding stages. The current method for assessing lines for vigour involve a visual score of lines on a one to nine scale taken pre canopy closure. This is somewhat subjective as different operators may interpret observations differently, and there can be issues as operators become tired in scoring large field trials. Other methods such as physical weighing of biomass samples are prohibitive in terms of resource use for large scale screening required in breeding. Remote sensing methods are more rapid, efficient and objective compared to conventional methods of vigour estimation. The collection of large and accurate datasets would then better facilitate the understanding of associations between this trait and grain yield across a range of environments.

Field pea is an interesting crop in which to apply vegetation indices, as breeding has led to the development of two highly divergent architectural ideotypes. Traditionally, field pea had long internodes and highly compounded leaves with limited tendrils, giving rise to "conventional" type field pea. Kielpinski and Blixt (1982) combined two recessive genes, *afila* and *length*. *afila* converts the compound leaf to an abundance of tendrils, while *length* reduces the length of the internodes. Together, these traits form the semi-dwarf, semi-leafless ideotype which has much better standability in the field, facilitating a much easier harvest. It is currently unknown how these traits affect vegetation indices and their relation to biomass accumulation.

Spectral VIs derived from active sensors as deployed in a CC and passive sensors such as the MicaSense RedEdge-M™ could be useful in a field pea breeding program. The objectives of this study were to (i) test ground and aerial-based remote sensing vegetation indices (VIs) for trait-based genotype variety selection, (ii) improve our understanding of the association between measured plant traits and readings derived from active and passive sensors and (iii) establish an optimal time for growth assessments in relation to field pea vigour and seed yield.

2. Materials and methods

2.1. Experimental site

Field experiments were conducted during the winter growing seasons between 2017 and 2020 (Table 1) at Beulah (36°03'36.0"S, 142°29'38.04"E) and Horsham (36°43'49.2"S 142°06'25.1"E and 36°44'10.8"S, 142°06'25.40"E) in Victoria and at Yenda (33°59'47.5"S, 146°08'32.2"E), Wagga Wagga (35° 2' 42.6408'' S, 147° 21' 3.0384'' E) and Ardlethan (34° 36' 32.6376'' S, 147° 6' 24.2028'' E) in New South Wales in Australia. The research sites of Victoria were characterized by Vertisol soil in Horsham and Calcareous soils in Beulah. The soil type of NSW was Chromic Luvisols. The rainfall was well below the 50-years average rainfall in 2019 in both regions. The conditions of the experimental sites are presented in Table 1.

2.2. Genotype description and field experiments

Three experiments were conducted over three consecutive years. Experiment 1 was conducted in 2017, 2018 and 2020 where forty-four varieties representing a range of important historical lines were evaluated in a RCBD trial replicated three times at Horsham. Datasets from this trial were used to validate non-destructive and destructive methods of measuring aboveground biomass and seed yield.

Experiment 2 was conducted at Horsham in 2019 and consisted of ten current varieties of field pea with three replicates in a randomized completed block design (RCBD) trial. Experiment 3 consisted of two replicate RCBD trials of two hundred and seventeen genotypes representing stage 2 breeding germplasm from the Australian national field pea breeding program. This trial was grown over five sites, namely Horsham and Beulah in Victoria and Yenda, Wagga Wagga and Ardelthan in New South Wales. Experiments 2 and 3 had eight varieties in common and represented 3 ideotypic classes on which detailed measures were taken. These ideotypes were (i) semi-dwarf, semi-leafless varieties and included PBA Oura, PBA Pearl, PBA Twilight, Kaspa and PBA Butler, (ii) a fully leaved short internode breeding line (OZP1604) and conventional or fully leaved varieties with long internodes (Sturt

Table 1
Experimental conditions at each site.

Experiment	No. of genotype	Date of planting	Year	Environment	Region	Soil type	In-crop Rain fall (mm)	Location GPS
1	44	08-Jun	2017	Horsham (E1)	VIC	Vertisol	253	36°43'49.2"S 142°06'25.1"E
1	44	14-May	2018	Horsham (E1)	VIC	Vertisol	151	36°44'10.8"S, 142°06'25.40"E
1	44	28-May	2020	Horsham (E1)	VIC	Vertisol	217	36°43'49.2"S 142°06'25.1"E
2	10	06-Jun	2019	Horsham (E1)	VIC	Vertisol	192	36°43'49.2"S 142°06'25.1"E
3	217	06-Jun	2019	Horsham (E1)	VIC	Vertisol	192	36°43'49.2"S 142°06'25.1"E
3	217	15-May	2019	Beulah (E2)	VIC	Calcareous	186	36°03'36.0"S, 142°29'38.04"E
3	217	08-May	2019	Yenda (E3)	NSW	Chromic luvisol	87	33°59'47.5"S, 146°08'32.02"E
3	217	22-May	2019	Wagga Wagga (E4)	NSW	Chromic luvisol	126	35°02'42.6''S, 147°21'03.03''E
3	217	14-May	2019	Ardlethan (E5)	NSW	Chromic luvisol	99	34°36'32.6''S, 147°06'24.02''E

Eight divergent ideotypes of field pea from Experiment 2 (Horsham, E1) and seven from Experiment 3 (Beulah, E2) were selected for detailed measurements. These ideotypes had three classes: (i) semi-dwarf, semi-leafless varieties (PBA Oura, PBA Pearl, PBA Twilight, Kaspa and PBA Butler), (ii) a fully leaved short internode breeding line (OZP1604) and (iii) conventional or fully leaved varieties with long internodes (Sturt and PBA Percy). Sturt was missing at the Beulah experimental site.

and PBA Percy). Sturt was missing at the Beulah experimental site.

All plots were 5 m long and consisted of five rows spaced 0.25 m apart. Plots had a 2 m gap within the ranges and a 0.5 m gap between the rows. Fertilizer and herbicides were applied according to best farmer practice for the region. Details of these experiments are presented in Table 1.

2.3. Plant measurements

The aboveground biomass was harvested from 0.5 m x 1.25 m at an early vegetative stage in experiment 1 and experiment 2, and twice more in experiment 1 coinciding with canopy closure and physiological maturity. Seed yield was harvested from 5 m x 1.25 m at physiological maturity from each plot of all three experiments.

Spectral reflectance readings were taken at up to 19 time points using the handheld CC configured with green, red and NIR channels (Model ACS-470, Holland Scientific, Inc). CC was also configured to take 10 samples readings per second. During measurements, the detection optics of the CC were positioned over the middle row of a 5-row plot at approximately 0.75 m height above canopy with a sensor field view of 32 degrees, resulting in a projected beam of 0.43 m width. This height is within the range recommended by the manufacturer to minimise soil spectrum effects (https://hollandscientific.com). Average reflectance values from approximately 20 readings were taken for each plot by walking at a consistent pace and taking measurement from the middle row along the 5 m plot length.

2.4. Aerial data acquisition

This research used a custom multispectral data acquisition system integrated for phenotypic research at SmartSense iHub, Agriculture Victoria, as described in Banerjee et al. (2020). The system consists of a MicaSense RedEdge-M multispectral camera (MicaSense, Seattle, WA, USA) integrated with the unmanned aerial vehicle (UAV) DJI Matrice 100 quadcopter at Horsham and Bask Aerospace MR4 (4 rotors) at Beulah. The multispectral sensor records the position values, i.e. latitude, longitude and altitude on to the camera tags, using the included global positioning system (GPS) module. Additionally, the multispectral camera also logs dynamic changes in incident irradiance levels using a downwelling light sensor. A radiometric calibration panel with known radiometric coefficients for individual multispectral bands was used. Radiometric calibration measurements were recorded with the multispectral sensor before individual flight missions for image correction.

Meticulous flight planning is important for UAV aerial data acquisition critical in high-throughput phenotyping. The UAV trajectory was designed using Ground Station Pro (DJI, Shenzhen, China) and the multispectral sensor was set to acquire images at a specified overlap (80% at Horsham and 75% at Beulah) and height (35 m at Horsham and 58 m at Beulah) to achieve a ground sampling distance (GSD) of 2 cm at Horsham and 4 cm at Beulah. The UAV-multispectral data was acquired at different days after sowing (DAS) to map the spectral profile of the cultivars over their life cycle. Strategic flights were carried out before destructive harvesting of biomass, to evaluate the benefit of utilizing UAV-multispectral systems as a high-throughput phenotypic tool at Horsham. Total flights of nine at Horsham and eleven at Beulah were conducted as detailed in Table 2.

2.5. UAV data processing

This study adopted the workflow developed in Banerjee et al. (2020), wherein the detailed workflow is provided. Here, we present a brief overview of the adopted workflow Fig. 1.

The acquired UAV multispectral images were processed using a photogrammetry software, Pix4D Mapper (Pix4D, 2017). The software used a technique called Structure from Motion (SfM) which is well-suited for processing UAV data to generate the reflectance orthomosaic, the digital surface model (DSM) and the digital terrain model (DTM) layers. The mosaicked layers were then exported to individual (.tif) files with a spatial resolution of 2 or 4 cm GSD.

The MicaSense RedEdge multispectral camera records reflectance in blue (475 nm), green (560 nm), red (668 nm), red edge (717 nm), and near-infrared (840 nm) bands. These surface reflectance values were used to compute a total of 12 VIs, used in plant phenotyping research (Table 3). These indices enhance the contribution of spectral properties of the vegetation to correct confounding factors such as reflectance of soil backgrounds in a crop, particularly at the early stages of the growth cycle (Xue and Su, 2017). Additionally, VIs are immune to operator bias or assumptions regarding land cover class, soil type, or climatic conditions (Banerjee et al., 2020), therefore improving objectivity of high-throughput phenotyping of crops.

A crop coverage (CCov) metric was also computed to classify vegetation fraction region, the vegetation part of the research plots, as described in Banerjee et al. (2020). The CCov layer provides a highly accurate (99.2% overall accuracy) means to classify the vegetation cover within each plot. CCov is effective in suppressing background soil spectrum to improve the detection of vegetation, which is important in early stages of crop growth when estimating emergence.

For each plot (i.e. footprint size of 1 m x 5 m) the VI and CCov layers were summarized as average of all pixel values in the plot. A shapefile (.shp) consisting of the individual field plot extent was prepared in ArcMap version 10.4.1 (Esri, Redlands, CA, United States). The image processing involved in computation of VIs and CCov were performed in Python 3.7.8 (Python Software Foundation. Python Language Reference).

Cumulative NDVI was computed in terms of area under the NDVI progress curve as in Eq. (1).

$$AUC = \sum_{i=1}^{n-1} \left[\frac{(x_{i+1} + x_i)}{2}\right] * [t_{i+1} + t_i] \quad (1)$$

Where,

Table 2
Details of UAV-multispectral data acquisition in Horsham (Experiment 2) and Beulah (Experiment 3).

Flight number	Date of acquisition	Flying Height	Overlap (%)	GSD	Flight speed (m/sec)	Local illumination conditions	UAV
UAV-flights at Horsham							
1	2019–07–19	35 m	80	2 cm	5	Sunny	
2	2019–07–31	35 m	80	2 cm	5	Overcast cloudy	
3	2019–08–14	35 m	80	2 cm	5	Patchy cloudy	
4	2019–08–27	35 m	80	2 cm	5	Patchy cloudy	
5	2019–09–03	35 m	80	2 cm	5	Overcast cloudy	DJI Matrice 100 quadcopter
6	2019–09–11	35 m	80	2 cm	5	Sunny	
7	2019–10–03	35 m	80	2 cm	5	Sunny	
8	2019–10–14	35 m	80	2 cm	5	Overcast cloudy	
9	2019–10–22	35 m	80	2 cm	5	Overcast cloudy	
UAV-flights at Beulah							
1	2019–07–24	58 m	75	4 cm	10	*	
2	2019–08–13	58 m	75	4 cm	10	*	
3	2019–08–16	58 m	75	4 cm	10	*	
4	2019–08–23	58 m	75	4 cm	10	*	
5	2019–08–27	58 m	75	4 cm	10	*	
6	2019–08–30	58 m	75	4 cm	10	*	Bask Aerospace MR4(4 rotors)
7	2019–09–04	58 m	75	4 cm	10	*	
8	2019–09–10	58 m	75	4 cm	10	*	
9	2019–09–14	58 m	75	4 cm	10	*	
10	2019–09–24	58 m	75	4 cm	10	*	
11	2019–10–12	58 m	75	4 cm	10	*	

* =data not recorded but cloud shadows were not detected across target areas.

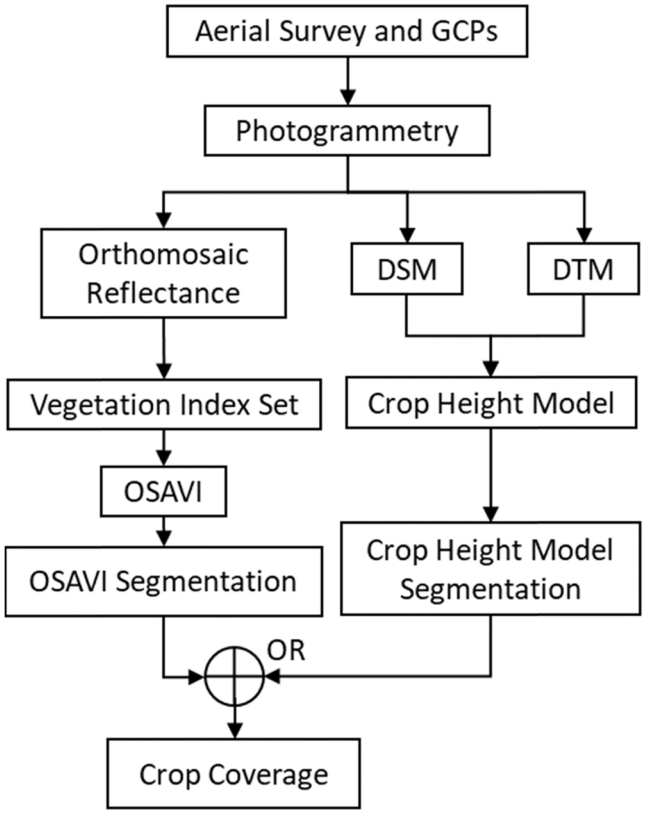

Fig. 1. The workflow ofUAV-multispectral data processing. GCPS=ground controlpoints, DSM=digital surface model, DTM=digital terrain model, OSAVI=optimizedsoil adjusted vegetation index.
(Adapted from Banerjee et al., 2020).

AUC is area under NDVI curve, x_i is NDVI at i^{th} day after sowing, t_i is the duration in days, n is the total number measurements.

2.6. Statistical analysis

The analysis of variance, additive main-effects and multiplicative interaction (AMMI) model and genotype main effect and genotype by environment interaction (GGE) biplot were computed using GenStat software package (VSN International, 2015). Further analysis using correlation and linear regression were analysed using Microsoft Excel.

3. Results

3.1. Ground and aerial-based sensors validation for NDVI

UAV derived NDVI was strongly and positively related to CC-NDVI (Fig. 2) at both Horsham (R^2 = 0.77; n = 210; p < 0.001; RMSE = 0.08) and Beulah (R^2 = 0.85; n = 1165; p < 0.001; RMSE = 0.20). A comparison between both sensors in detecting differences in each genotype was also made using the dataset of 2019 (Experiment 2). Aerial NDVI was highly and significantly correlated to ground based NDVI in all lines (Fig. 3).

3.2. NDVI based variety rankings across locations and crop growth stages

The difference between a near-infrared band of light and a visible light band of light as measured by NDVI was used for trait-based genotype rankings. Fig. 4 presents the readings of the NDVI of eight and seven varieties of field pea at multiple time points at Horsham and Beulah, respectively. The readings were taken using both CCand UAV from an early vegetative growth stage to senescence of the field pea. The plot based NDVI increased with time towards canopy closure. The highest mean saturation values were reached at 111 DAS using CC-NDVI (0.83) and at 118 DAS using UAV-NDVI (0.85) at Horsham, whereas the NDVI values reached the peak at 106 DAS using CC-NDVI (0.67) and at 127 DAS using UAV-NDVI (0.79) at Beulah for the variety PBA Percy.

Based on a time series analysis, there were statistically significant differences among the varieties for NDVI readings (Sup Table 1) before canopy closure (up to 101 DAS). Generally speaking, the conventional varieties of PBA Percy and Sturt had higher NDVI readings (Sup Table 1) and cumulative area under NDVI curve (Fig. 4) than that of most semi-dwarf, semi-leafless varieties with the most obvious exception of PBA Twilight. Additionally, the NDVI values of PBA Twilight were significantly higher than that of semi-leafless varieties, viz., OZP1408, PBA Butler, PBA Pearl and PBA Oura (Sup Table 1) during the early vegetative stage of crop development to canopy closure. PBA Twilight also had a larger area under the NDVI curve when compared to other semi-

Table 3
Spectral reflectance vegetation indices used in this study.

Name of Indices	Abbrev.	Formula	Reference
Normalized Difference Vegetation Index	NDVI	$\frac{(\rho NIR - \rho RED)}{(\rho NIR + \rho RED)}$	Rouse et al. (1974)
Green Normalized Difference Vegetation Index	GNDVI	$\frac{(\rho NIR - \rho GREEN)}{(\rho NIR + \rho GREEN)}$	Gitelson et al. (1996)
Enhanced Vegetation Index	EVI	$\frac{2.5(\rho NIR - \rho RED)}{(\rho NIR + 6*\rho RED - 7.5*\rho Blue + 1)}$	Huete et al. (2002)
Normalized Difference RedEdge Index	NDREI	$\frac{(\rho NIR - \rho RED\ EDGE)}{(\rho NIR + \rho RED\ EDGE)}$	Gitelson and Merzlyak (1994)
Chlorophyll Index RedEdge	CIRE	$\frac{(\rho NIR)}{(\rho RED\ EDGE)} - 1$	Gitelson et al. (2003)
Green Leaf Index	GLI	$\frac{(2*\rho GREEN - \rho RED - \rho Blue)}{(2*\rho GREEN + \rho RED + \rho Blue)}$	Lohaaichi et al. (2001)
Optimized soil adjusted vegetation index	OSAVI	$1.6[\frac{(\rho NIR - \rho RED)}{(\rho NIR + \rho RED + 0.16)}]$	Rondeaux et al. (1996)
Modified simple ratio	MSR	$\frac{(\rho NIR/\rho RED) - 1}{\sqrt{(\rho NIR/\rho RED)} + 1}$	Chen et al. (2014)
Modified chlorophyll absorption ratio index 1	MCARI1	$1.2[2.5(\rho NIR - \rho GREEN) - 1.3(\rho RED - \rho GREEN)]$	Haboudane et al. (2004)
Modified chlorophyll absorption ratio index 2	MCARI2	$\frac{3.75(\rho NIR - \rho RED) - 1.95(\rho NIR - \rho GREEN)}{(2*\rho NIR + 1)^2 - (6*\rho NIR + 5\sqrt{\rho RED}) - 0.5}$	Haboudane et al. (2004)
Modified triangular vegetation index 1	MTVI1	$1.2[2.5(\rho NIR - \rho GREEN) - 2.5(\rho RED - \rho GREEN)]$	Haboudane et al. (2004)
Modified triangular vegetation index 2	MTVI2	$\frac{1.8(\rho NIR - \rho GREEN) - 3.75(\rho RED - \rho GREEN)}{\sqrt{(2*\rho NIR + 1)^2 - (6*\rho NIR + 5\sqrt{\rho RED}) - 0.5}}$	Haboudane et al. (2004)
Pigment specific simple ratio for chlorophyll a	PSSRA	$\frac{(\rho NIR)}{(\rho RED)}$	Blackburn (1998)

leafless varieties (Fig. 5). Furthermore, conventional varieties with longer internodes (PBA Percy & Sturt) had higher and significant pre- and post-canopy closure NDVI values than the conventional short internode, OZP1604 line. In contrary, significant differences among genotype were not observed in terms of destructive measurement of biomass at two sample points (Sup Table 1). The non-destructive method was more sensitive in detecting phenotypic variation at these time points.

The study found good correlations between biomass and UAV derived NDVI measures within the idiotypic classes at $P < 0.05$ in the semi-dwarf, semi-leafless class ($r = 0.71$) and in the conventional leaved ($r = 0.99$) class. However, the correlation was not significant when all classes were combined.

3.3. Vegetation index-based estimation of biomass

A relationship between biomass and vegetation indices of field pea was also studied in Experiments 1 and 2 at Horsham (Fig. 6a and b). Aboveground biomass production was linearly related to various vegetation indices derived from a multi-spectral camera mounted on a UAV (Fig. 6a). In addition, CC- NDVI was positively linked to biomass ($R^2 = 0.60$, $p < 0.001$, RMSE=144.6 g) in field pea (Fig. 6b). Comparing a range of spectral indices, it was found that normalized difference red-edge index (NDREI) gave the highest correlations to aboveground biomass with a high coefficient of determination ($R^2 = 0.94$) (Fig. 6a).

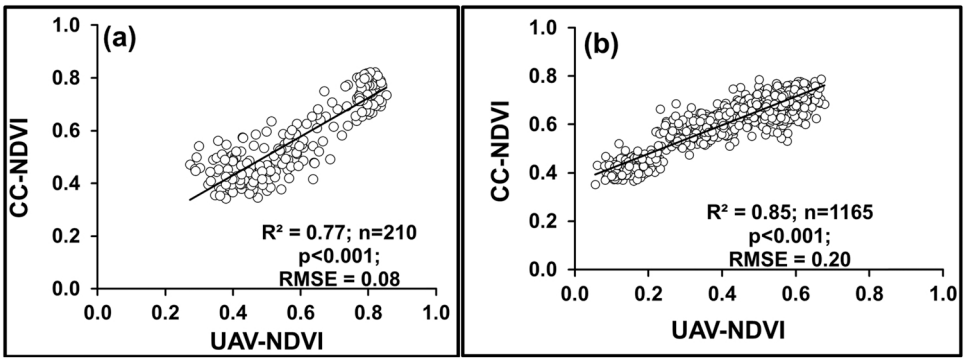

Fig. 2. NDVI readings of field pea varieties using handheld crop circle and UAV at Horsham (a) and at Beulah (b) in 2019 (experiments 2 & 3).

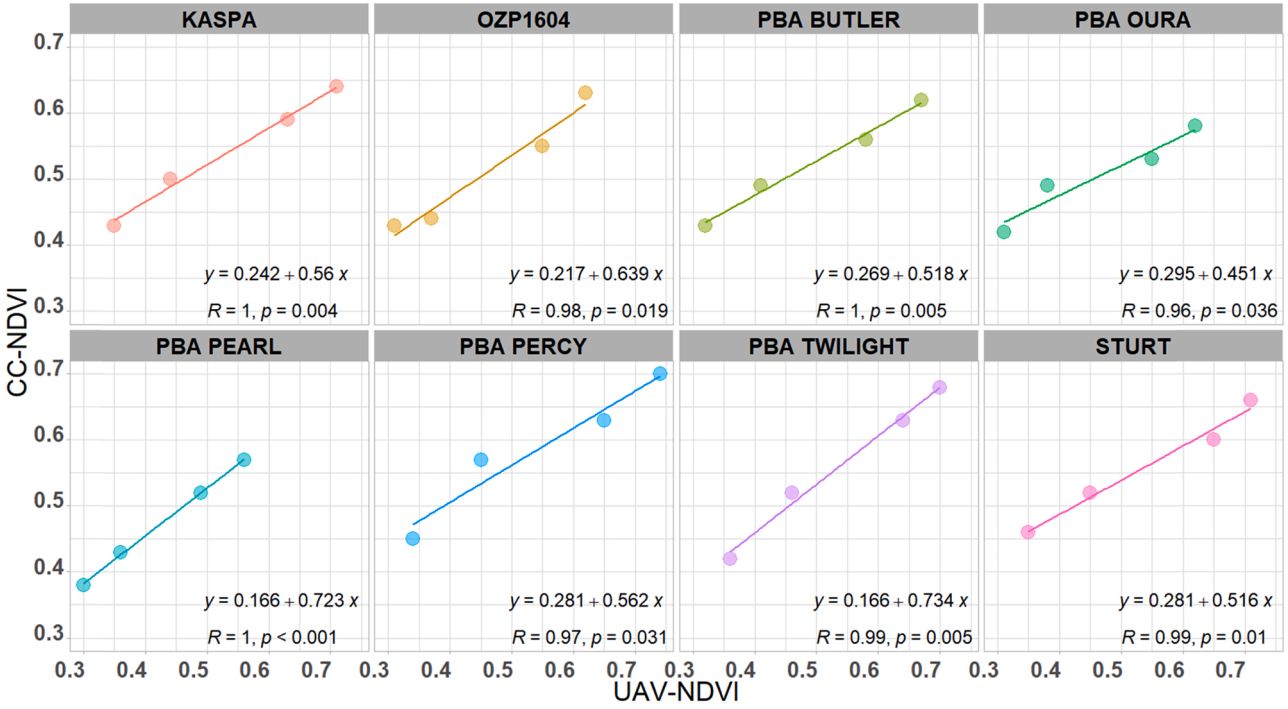

Fig. 3. The relationship between NDVI derived from Crop Circle (CC-NDVI) and UAV of eight varieties of field pea at Horsham in 2019 (experiments 2). Data was from four sampling points at pre-canopy closure (i.e. CC-NDVI at 60, 68, 89, 94 & UAV-NDVI at 54, 68, 88, 96 days after sowing).

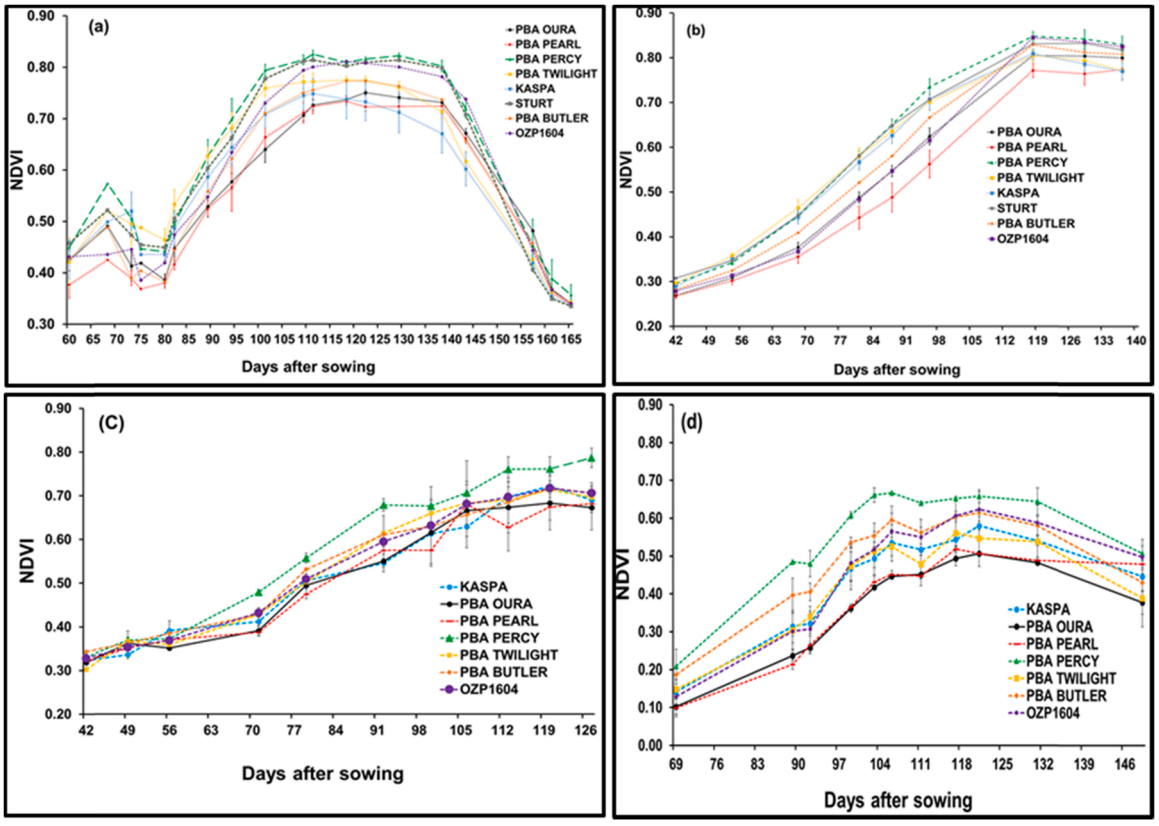

Fig. 4. Plot level NDVI mean of field pea varieties using handheld crop circle (a, c) and UAV (b, d) at Horsham (a, b) and Beulah (c, d) in 2019 cropping season (experiment 2 = a & b & experiment 3 =c & d).

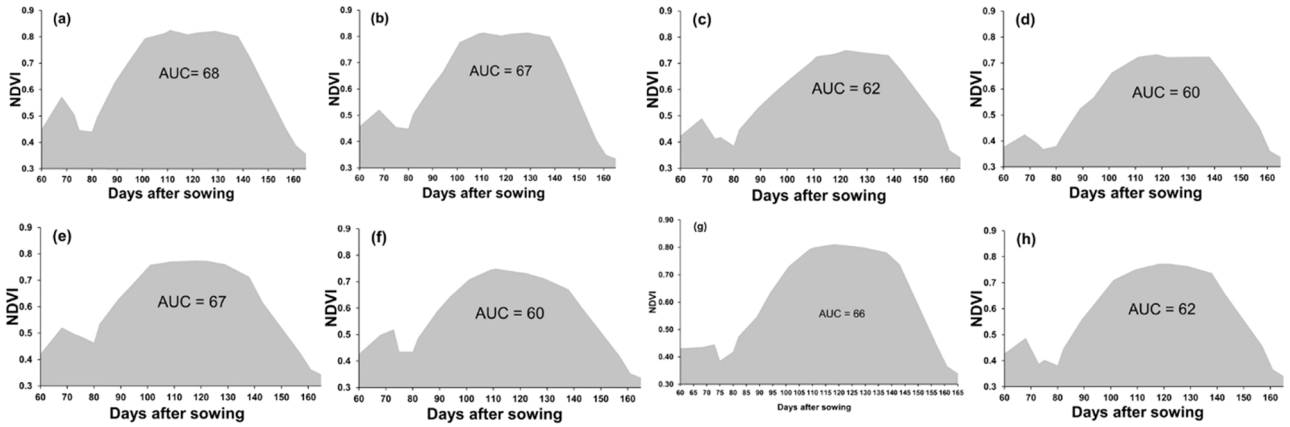

Fig. 5. The area under the NDVI curve based on data from crop circle at Horsham in 2019 (experiment 2). AUC is the area under the NDVI curve, a=PBA Percy, b=Sturt, c=PBA Oura, d=PBA Pearl, e = PBA Twilight, f = Kaspa, g = OZP1604, h = PBA Butler (experiment 2).

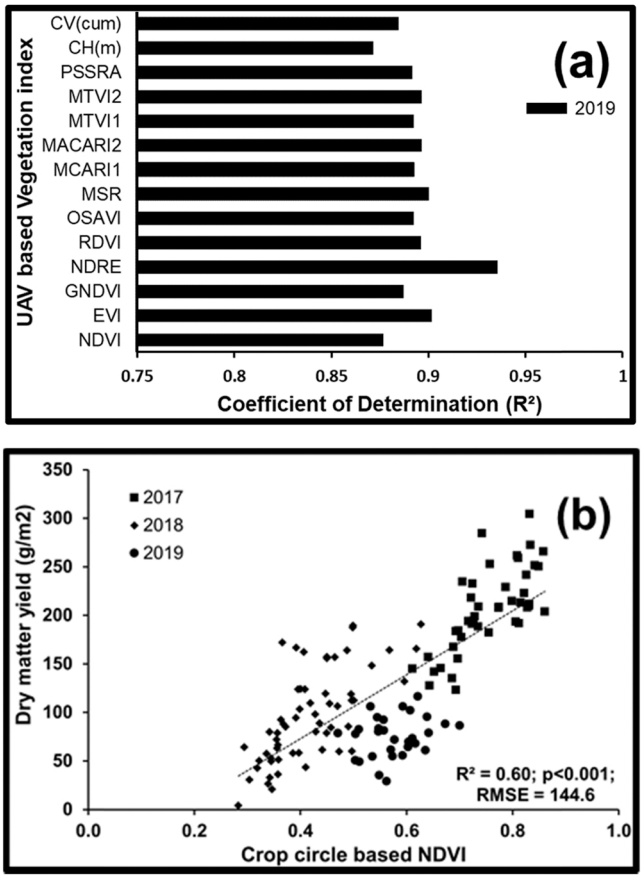

Fig. 6. Relationships between UAV (a) and Crop Circle (b) derived vegetation indices and aboveground biomass yields at early growth stage of field pea at Horsham experimental site (Fig. 6a=Experiments 2 and Fig. 6b=experiments 1 & 2). NDVI = Normalized Difference Vegetation Index, GNDVI=Green Normalized Difference Vegetation Index, EVI = Enhanced Vegetation Index, NDREI = Normalized Difference RedEdge Index, CV = Crop Volume (cumulative), CH = Crop Height, RDVI= Renormalized Difference Vegetation Index, OSAVI= Optimized Soil Adjusted Vegetation Index, MCARI1 = Modified Chlorophyll Absorption Ratio Index 1, MCARI1 =Modified Chlorophyll Absorption Ratio Index 2, MTVI1 = Modified Triangular Vegetation Index1, MTVI2 = Modified Triangular Vegetation Index2, PSSRA= Pigment Specific Simple Ratio for chlorophyll a.

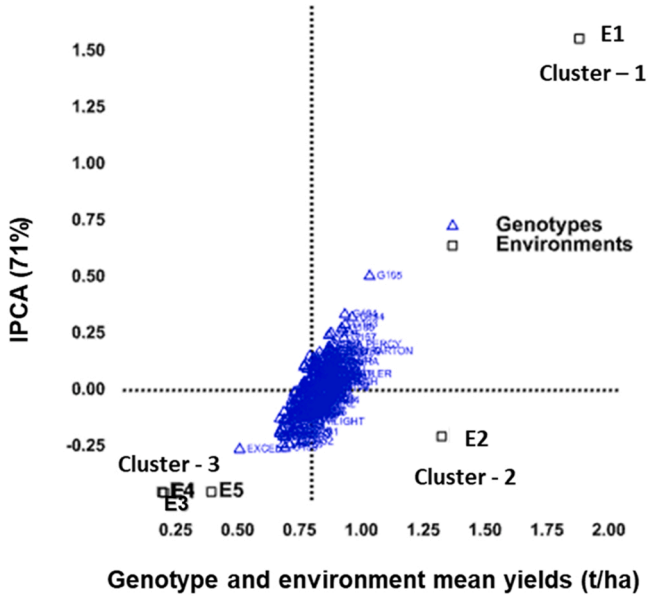

Fig. 7. AMMI biplot based genotype and environment clustering using seed yield of two hundred seventeen genotypes (G1 – G217) in five environments (E1 - E5). E1 = Horsham, E2 = Beulah, E3 = Ardlethan, E4 = Wagga Wagga, E5 = Yenda (experiment 3).

3.4. Interrelationships between seed yield and vegetation indices

In a breeding program, high yielding and consistent genotypic performances across production environments are desirable for wide adaptation. However, some genotypes are adapted to specific environments due to genotype by environment interaction (GEI) effects. In this study we clustered the field pea trials into relatively homogenous environments using AMMI and GGE analysis. As illustrated in Figs. 7 and 8, both AMMI and GGE clearly classified production environments into three distinctive potential environments using 270 genotypes in five environments (experiment – 3). The AMMI model grouped the low yielding environments into cluster 3 and the high yielding environments into cluster 1 and cluster 2 (Fig. 7). The GGE model used six lines and divided the biplot into six sectors of the convex hull (Fig. 8). The low yielding environments (E3 = Ardlethan, E4 = Wagga Wagga and E5 = Yenda) fell into one sector while the other two high yielding environments (E1 = Horsham and E2 = Beulah) fell into two of the six sectors. Overall, the environments were clustered into three mega environments using both AMMI and GGE. The mega environments were

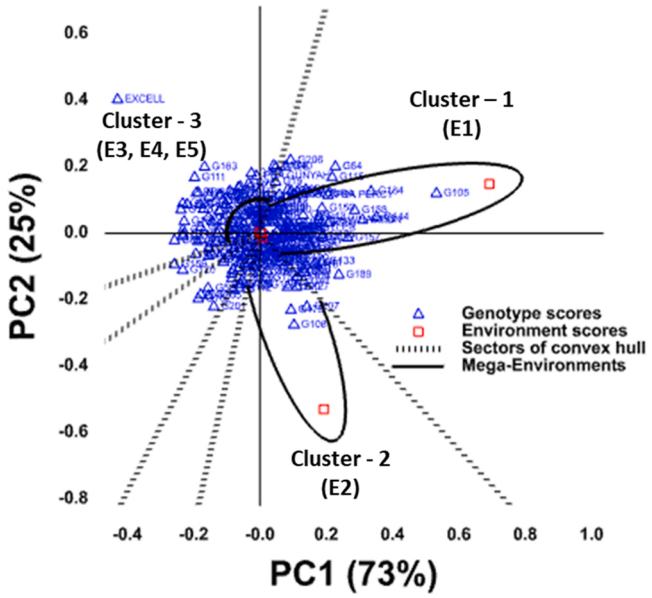

Fig. 8. GGE biplot based genotype and environment clustering using seed yield of two hundred seventeen genotypes (G1 – G217) in five environments (E1 - E5). E1 = Horsham, E2 = Beulah, E3 = Ardlethan, E4 = Wagga Wagga, E5 = Yenda (experiment 3).

Table 4
Pearson correlations between cumulative area under NDVI measures derived from either UAV or crop circle in two main divergent architectural ideotypes.

Type	UAV-NDVI	CC-NDVI
SD-SL (7)	0.71 * **	0.41
Conventional (3)	0.99 * **	-0.45
All (10)	0.29	0.08

Three conventional leaved varieties and seven semi-dwarf, semi-leafless (SD-SL) varieties were included from dataset of 2019 (Experiment 2).

Table 5
The first three AMMI selections per environment.

Environment	Region	yield (t/ha)	Selection-1	Selection-2	Selection-3
Horsham (E1)	VIC	1.88	G105	G184	G144
Beulah (E2)	VIC	1.32	G108	G207	G179
Yenda (E3)	NSW	0.39	PBA Percy	G129	G38
Wagga Wagga (E4)	NSW	0.19	PBA Percy	G38	G129
Ardlethan (E5)	NSW	0.20	PBA Percy	G38	G143

In this study, two hundred seventeen genotypes (G1 – G217) in five environments (E1 - E5) were used in 2019. E1 = Horsham, E2 = Beulah, E3 = Ardlethan, E4 = Wagga Wagga, E5 = Yenda (experiment 3).

defined by drawing an ellipse around environments located in the same sector. The clustering results were consistent with rainfall received during the 2019 winter cropping season (Table 1) and subsequent yields (Table 5).

Further analysis based on both AMMI and GGE biplot clustering was carried out to identify traits of specific adaptation in relation to seed yield under two contrasting production environments. Using the AMMI model, genotypes were clustered based on their adaptability to diverse environments (experiment 3). For example, the model identified a variety with high vigour (PBA Percy, for example) as the most adaptive to low yielding environments (Table 5). The model also identified G105 and G108 as the most adaptive genotypes in the high yielding environments (Table 5).

In the high yielding environments (E1), seed yield was negatively related to several vegetative indices (VIs) derived from both CC and UAV at an early growth stage (experiment 2). During post-flowering or post canopy closure, there was a positive association between seed yield and VIs derived from UAV though the relationship was not statistically significant (Fig. 9).

In the low yielding environments (E3, E4 & E5), seed yield was significantly related to NDVI during the early growth stage of field pea (i.e. 28 days after sowing). Varieties with high vigour scores (NDVI readings) were high yielding in a low yielding environment (in-crop rainfall < 126 mm) (Fig. 10a). On the contrary, low vigour varieties were high yielding in high yielding environment (in-crop rainfall > 186 mm) (Fig. 10b, c and d).

4. Discussion

Development of high-yielding varieties requires an assessment of a large number of breeding lines to select for a range of desirable traits. Visual scoring and physical measurements for desirable traits are usually carried out on hundreds of breeding plots. However, quantification of these traits are generally labour intensive, can be somewhat subjective and expensive (Potgieter et al., 2017). Sensors and multispectral image-based measurements could be an effective and accurate method for large scale germplasm screening for multiple traits in field pea.

The current studies found that both active (CC) and multispectral passive sensors (UAV-deployed) showed similar NDVI trends in genotype rankings in terms of various parameters in most cases. This was in spite of there being a large difference in the footprint size of the two sensing technologies. CC measured a width of 0.43 m over the 5 m plot length, which essentially only covered the middle row in a 5 row plot (row spacings were 0.25 m) while processing of UAV images took readings from all 5 rows in the plot. These different footprints of the technologies indicates that although the percentage of soil spectra likely varied between CC and UAV derived measurements, such effects were proportional between varieties and did not affect the final results.

Vegetation indices have been proposed as a means of non-destructive biomass assessment in screening large numbers of germplasm for vigour. In this study, biomass was strongly and significantly related to NDVI. This is particularly useful to rapidly and effectively measure early vigour in diverse field pea germplasm. However, there was a difference between NDVI of both sensors in relation to biomass production in the two architectural ideotypes of pea. A significant correlation was found between biomass and cumulative area under UAV-NDVI, however, no significant correlation was found for CC-NDVI at a single time point. As previously stated, NDVI measurements using CC only measured a single row whereas the UAV mounted sensor measured the whole plot. It seems the UAV readings had greater accuracy and likely had a greater proportion of green biomass to soil than the ground-based measures.

Early vigour is commonly measured by NDVI derived from ground-based and aerial-based sensors and is considered as a surrogate of biomass production (Duan et al., 2017). It has been reported that early vigour traits such as leaf expansion rate (Mullan and Reynolds, 2010), dry matter production (Cowley et al., 2014; Li et al., 2010; Diepenbrock, 2000) and increased crop growth rate (Mullan and Reynolds, 2010) are linked to grain yield (Cowley et al., 2014; Zhou et al., 2007; Botwright et al., 2002; Kumar et al., 2009; Rebetzke and Richards, 1999). In low rainfall environments, these desirable traits are essential to improve the water use efficiency of field crops through rapid canopy closure, which increases water availability by reducing water loss to evaporation.

Previous studies have used NDVI to estimate early vigour in many crops (Cowley et al., 2014; Holzapfel et al., 2009; Basnyat et al., 2004). Studies on canola showed a significant correlation (r = 043–0.80) between early vigour (as measured by NDVI) and seed yield (Cowley et al., 2014; Holzapfel et al., 2009; Basnyat et al., 2004). These studies suggested the optimal time to measure NDVI to predict canola seed yields was between 44 and 79 days after sowing (Cowley et al., 2014; Basnyat

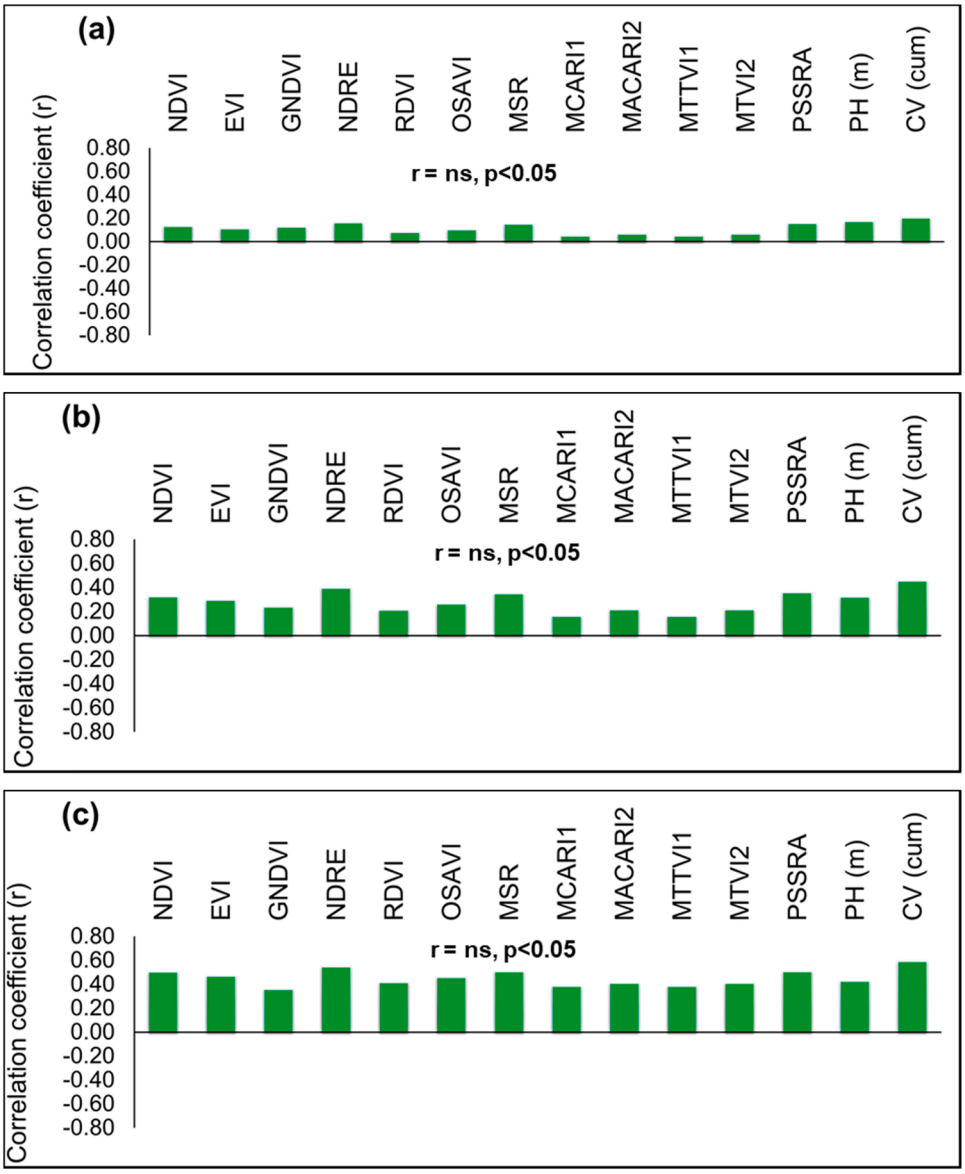

Fig. 9. Relationships between seed yield and UAV derived vegetation indices at multiple growth stages of field pea at Horsham in 2019 (experiment 2). a= 118 DAS, b= 129 DAS, c= 137 DAS. NDVI = Normalized Difference Vegetation Index, GNDVI=Green Normalized Difference Vegetation Index, EVI = Enhanced Vegetation Index, NDREI = Normalized Difference RedEdge Index, RDVI= Renormalized Difference Vegetation Index, OSAVI= Optimized Soil Adjusted Vegetation Index, MCARI1 = Modified Chlorophyll Absorption Ratio Index 1, MCARI1 =Modified Chlorophyll Absorption Ratio Index 2, MTVI1 = Modified Triangular Vegetation Index1, MTVI2 = Modified Triangular Vegetation Index2, PSSRA= Pigment Specific Simple Ratio for Chlorophyll a, CH=Crop Height, CV=Crop Volume.

et al., 2004). Studies on wheat also found strong positive correlations between grain yield and NDVI measurement taken at flowering (Duan et al., 2017), milky stage (Babar et al., 2006) and grain filling (Sultana et al., 2014). Our study mainly found negative correlations between seed yield and NDVI during early growth stages of pea in high yielding environments. Vegetation indices derived from UAV (NDVI, EVI, GNDVI, NDRE, RDVI, OSAVI, MSR, MCARI1, MACRI2, MTVI1, MTVI2, PSSRA) including UAV estimated plant height during the reproductive stage (96 – 137 DAS) were positively related to seed yield in high yielding environments. Pandey et al. (2016) also reported a positive and significant relationship between seed yield and biomass (as measured by canopy cover) during the reproductive stage of canola in similar environmental conditions.

Further analysis using seed yield and NDVI data from five environments indicated an association between seed yield and early vigour (or NDVI reading) under water-limiting environments. We have demonstrated this using graphical illustrations by using both AMMI and GGE models. For example, no significant relationship was obtained between seed yield and vigour scores (or NDVI readings) under high rainfall environments, whereas under low rainfall environments, varieties with higher vigour scores produced better seed yield and this is in agreement with the canola work by Pandey et al. (2016). The lack of advantage of early vigour in a high potential environment could be due to the availability of adequate resources, mainly rainfall during the study period in Victoria compared to New south Wales.

Season to season climates are highly variable in Victoria and New South Wales and the current seed yield increase coupled with high early vigour in water-limited environments was likely caused by reduced water loss from increased ground cover at early crop development. For example, studies by Turner and Nicolas (1998) and Mullan and Reynolds (2010) have shown low soil evaporation rates under higher vigour wheat canopies in water-limiting environments. This relates to water use efficiency where reduced evaporation allowed greater water capture by the plant to produce grain. This is only effective in water-limiting environments. In the current study the seed yield was strongly associated with in-crop rainfall (R^2 =0.82, $p < 0.001$) (Tables 1 and 4), where early vigour was positively related to seed yield in direr environments. The advantage of early vigour traits as an adaptive response to drought has been widely reported in several studies (Nguyen et al., 2018; Cowley et al., 2014; Kumar et al., 2009; Zhou et al., 2007; Botwright et al., 2002; Rebetzke and Richards, 1999). Similarly, specific traits, such as deep root systems, shifting sowing time and genetic manipulation of crop

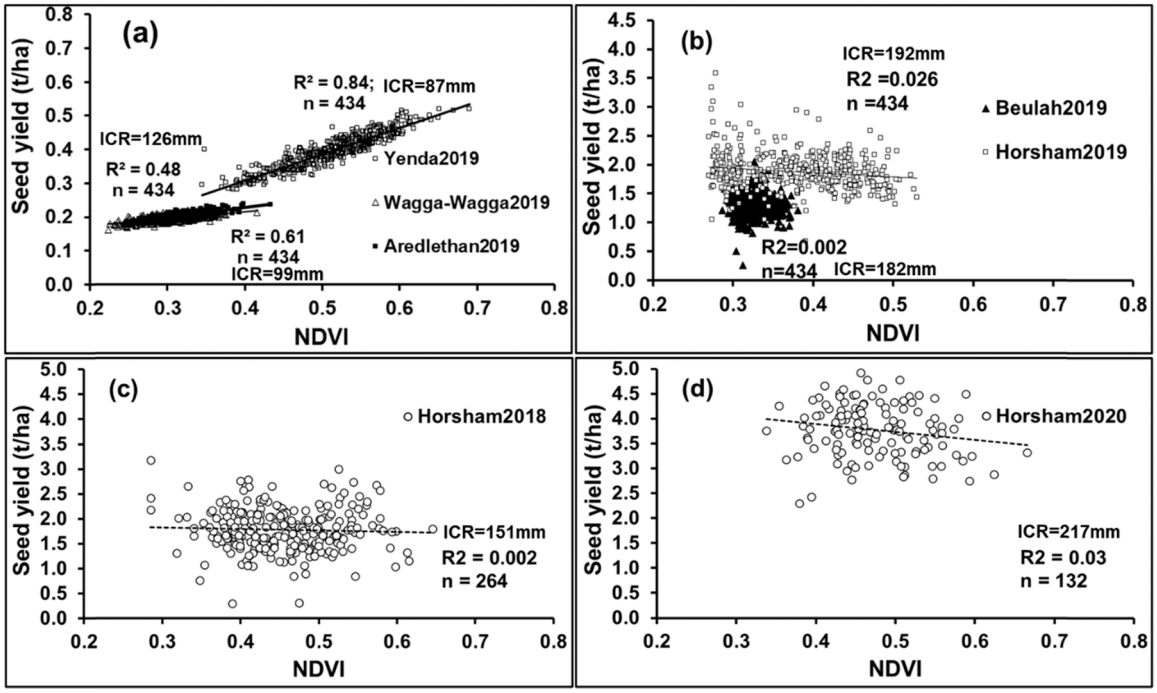

Fig. 10. Relationship between early vigour (NDVI readings) and yield of field peas in low (a) and high (b, c, d) yield potential environments (Fig. 10a &b = experiment 3 (Table 1); Fig. 10c & d=experiment 1(Table 1). n = number of observations, ICR=in-crop rainfall.

phenology have been suggested as means for improving water stress adaptation (Sadras et al., 2012; Manschadi et al., 2008). This result has demonstrated the potential of reflectance indices to predict final seed yield in field pea under specific conditions. Overall, the capability enables field pea breeders to screen a large number of breeding lines more rapidly and efficiently than the conventional destructive methods.

Architectural and morphological driven differences in early vigour were also detected using sensors deployed in field pea. During both pre and post-canopy closure, fully leaved varieties with long internodes (PBA Percy and Sturt) had significantly higher NDVI readings than OZP1604, a fully leaved short internode variety. Additionally, the long-internode pea generally had higher measures than the remaining short-internode, semi-leafless types. This latter plant type has an erected growth habit with an abundance of tendrils instead of leaves, as compared to the leafy prostrate conventional types. This data suggests that long internodes play a greater role in achieving canopy closure than the fully leaved trait, although a more balanced data set should be investigated to confirm this.

In addition, higher NDVI values were recorded at post canopy closure using CC than UAV. We also found low phenotypic variation among varieties of field pea between CC-NDVI and UAV-NDVI at Beulah. However, this could be due to a lower number of corresponding measurements at Horsham (n = 210) compared to Beulah (n = 1165), indicating that a greater number of measurements are likely to improve the R^2 between CC-NDVI and UAV-NDVI at Horsham. Neverthless, the relationship was found sufficiently strong for application in pea breeding research.

5. Conclusion

In this study, spectral reflectance vegetation indices derived from both CC (active sensor) and multispectral UAV (passive sensor) were capable of ranking field pea varieties for VIs related to vigour. The values of vegetation indices derived from both UAV and CC were strongly related to aboveground biomass yield at an early stage of field pea growth. We were also able to rank genotypes using area under the NDVI curve. The current study has also improved our understanding of the influence of morphological traits on NDVI readings during pre-and post-canopy closure. Our data shows that NDVI accurately reflect biomass accumulation within the semi-dwarf, semi-leafless class but this correlation broke down when conventional types were included. This indicates that AUC NDVI can only be used to assess biomass accumulation within the two classes of germplasm. The current study has also demonstrated the optimal timing and vegetation index to be used for final seed yield prediction in field pea. Given the in-crop rainfall being less than 126 mm, the optimal regime to conduct high-throughput measurements for best prediction of seed yield from early vigour is 28 days after sowing. Furthermore, vegetation indices in conjunction with environmental clustering using both AMMI and GGE biplots could be useful to identify traits with specific adaptation. The study also found early vigour as an important plant character in a drier environment to increase seed yield in field pea.

Declaration of Competing Interest

The authors declare that they have no known competing financial interests or personal relationships that could have appeared to influence the work reported in this paper.

Acknowledgement

This study was funded by Grain Research and Development Corporation (GRDC), Australia (DAV1607-010BLX), PulseBio3 Stable grain yield in pulses through improved stress tolerance and we greatly acknowledge the Corporation for supporting this work. We also thank the Molecular Plant Breeding team of Horsham Grain Innovation Park for their technical support.

Appendix A. Supporting information

Supplementary data associated with this article can be found in the online version at doi:10.1016/j.fcr.2021.108407.

References

Basnyat, P., McConkey, B., Lafond, G.P., Moulin, A., Pelcat, Y., 2004. Optimal time for remote sensing to relate to crop grain yield on the Canadian prairies. Can. J. Plant Sci. 84, 97–103. https://doi.org/10.4141/P03-070.

Banerjee, B.P., Spangenberg, G., Kant, S., 2020. Fusion of spectral and structural information from aerial images for improved biomass estimation. Remote Sens. 12, 3164. https://doi.org/10.3390/rs12193164.

Bhattarai, G.P., Schmid, R.B., McCornack, B.P., 2019. Remote sensing data to detect hessian fly infestation in commercial wheat fields. Sci. Rep. 9, 6109. https://doi.org/10.1038/s41598-019-42620-0.

Babar, M.A., Reynolds, M.P., van Ginkel, M., Klatt, A.R., Raun, W.R., Stone, M.L., 2006. Spectral reflectance to estimate genetic variation for in-season biomass, leaf chlorophyll, and canopy temperature in wheat. Crop Sci. 46, 1046–1057. https://doi.org/10.2135/cropsci2005.0211.

Beck, P.S.A., Atzberger, C., Høgda, K.A., Johansen, B., Skidmore, A.K., 2006. Improved monitoring of vegetation dynamics at very high latitudes: a new method using MODISNDVI. Remote Sens. Environ. 100, 321–334. https://doi.org/10.1016/j.rse.2005.10.021.

Beisel, N.S., Callaham, J.B., Sng, N.J., Taylor, D.J., Paul, A.L., Ferl, R.J., 2018. Utilization of single-image normalized difference vegetation index (SI-NDVI) for early plant stress detection. Appl. Plant Sci. 6 (10), e1186 https://doi.org/10.1002/aps3.1186.

Botwright, T.L., Condon, A.G., Rebetzke, G.J., Richards, R.A., 2002. Field evaluation of early vigour for genetic improvement of grain yield in wheat. Aust. J. Agric. Res 53, 1137–1145. https://doi.org/10.1071/AR02007.

Condorelli, G.E., Maccaferri, M., Newcomb, M., Andrade-Sanchez, P., White, J.W., French, A.N., Sciara, G., Ward, R., Tuberosa, R., 2018. Comparative aerial and ground based high throughput phenotyping for the genetic dissection of NDVI as a proxy for drought adaptive traits in durum wheat. Front. Plant Sci. 9, 893. https://doi.org/10.3389/fpls.2018.00893.

Cowley, R.B., Luckett, D.J., Moroni, J.S., Diffey, S., 2014. Use of remote sensing to determine the relationship of early vigour to grain yield in canola (Brassica napus L.) germplasm. Crop Pasture Sci. 65, 1288–1299. https://doi.org/10.1071/CP14055.

Diepenbrock, W., 2000. Yield analysis of winter oilseed rape (*Brassica napus* L.): a review. Field Crops Res. 67, 35–49. https://doi.org/10.1016/S0378-4290(00)00082-4.

Duan, T., Chapman, S.C., Guo, Y., Zheng, B., 2017. Dynamic monitoring of NDVI in wheat agronomy and breeding trials using an unmanned aerial vehicle. Field Crops Res. 210, 71–80. https://doi.org/10.1016/j.fcr.2017.05.025.

Erdle, K., Mistele, B., Schmidhalter, U., 2011. Comparison of active and passive spec-tral sensors in discriminating biomass parameters and nitrogen status in wheatcultivars. Field Crops Res. 124, 744–784. https://doi.org/10.1016/j.fcr.2011.06.007.

French J., R., 2010. The risk of vegetative water deficit in early-sown faba bean (Vicia faba L.) and its implications for crop productivity in a Mediterranean-type environment. Crop Pasture Sci. 61, 566–577. https://doi.org/10.1071/CP09372.

Gitelson, A.A., Kaufman, Y.J., Merzlyak, M.N., 1996. Use of a green channel in remote sensing of global vegetation from EOS-MODIS. Remote Sens. Environ. 58 (3), 289–298. https://doi.org/10.1016/S0034-4257(96)00072-7.

Gitelson, A., Merzlyak, M.N., 1994. Quantitative estimation of chlorophyll-a using reflectance spectra: Experiments with autumn chestnut and maple leaves. J. Photochem. Photobiol. B 22 (3), 247–252. https://doi.org/10.1016/1011-1344(93)06963-4.

Gitelson, A.A., Gritz, Y., Merzlyak, M.N., 2003. Relationships between leaf chlorophyll content and spectral reflectance and algorithms for non-destructive chlorophyll assessment in higher plant leaves. J. Plant Physiol. 160 (3), 271–282. https://doi.org/10.1078/0176-1617-00887.

Gupta, P.K., Balyan, H.S., Gahlaut, V., Kulwal, P.L., 2012. Phenotyping, genetic dissection, and breeding for drought and heat tolerance in common wheat: status and prospects. Plant Breed. Rev. 36, 85–168. https://doi.org/10.1002/9781118358566.ch2.

Leuning, R., Condon, A.G., Dunin, F.X., Zegelin, S., Denmead, O.T., 1994. Rainfall interception and evaporation from soil below a wheat canopy. Agric. For. Meteorol. 67, 221–238. https://doi.org/10.1016/0168-1923(94)90004-3.

Hatfield, J.L., Gitelson, A.A., Schepers, J.S., Walthall, C.L., 2008. Application of spectral remote sensing for agronomic decisions. Agron. J. 100, S-117–S-131. https://doi.org/10.2134/agronj2006.0370c.

Holzapfel, C.B., Lafond, G.P., Brandt, S.A., Bullock, P.R., Irvine, R.B., Morrison, M.J., May, W.E., James, D.C., 2009. Estimating canola (*Brassica napus* L.) yield potential using an active optical sensor. Can. J. Plant Sci. 89, 1149–1160. https://doi.org/10.4141/CJPS09056.

Huang, Y., Reddy, K.N., Fletcher, R.S., Pennington, D., 2018. UAV low-altitude remote sensing for precision weed management. Weed Technol. 32, 2–6. https://doi.org/10.1017/wet.2017.89.

Kielpinski, M., Blixt, S., 1982. The evaluation of the "Afila" character with regard to its utility in new cultivars of dry pea. Agric. Hort. Genet 40, 51–74.

Kim, S.L., Kim, N., Lee, H., et al., 2020. High-throughput phenotyping platform for analyzing drought tolerance in rice. Planta 252, 38. https://doi.org/10.1007/s00425-020-03436-9.

Kumar, A., Verulkar, S., Dixit, S., Chauhan, B., Bernier, J., Venuprasad, R., Zhao, D., Shrivastava, M.N., 2009. Yield and yield-attributing traits of rice (Oryza sativa L.) under lowland drought and suitability of early vigor as a selection criterion. Field Crops Res. 114, 99–107. https://doi.org/10.1016/j.fcr.2009.07.010.

Manschadi, A.M., Hammer, G.L., Christopher, J.T., deVoil, P., 2008. Genotypic variation in seedling root architectural traits and implications for drought adaptation in wheat (Triticum aestivum L.). Plant Soil 303, 115–129. https://doi.org/10.1007/s11104-007-9492-1.

Maydup, M.L., Graciano, C., Guiamet, J.J., Tambussi, E.A., 2012. Analysis of early vigour in twenty modern cultivars of bread wheat (Triticum aestivum L.). Crop Pasture Sci. 63, 987–996. https://doi.org/10.1071/CP12169.

Mir-Mahmoodi, T., Soleimanzadeh, H., 2009. Relationship between rapid canopy closure and grain yield in wheat. Asian J. Plant Sci. 8, 250–253. https://doi.org/10.3923/ajps.2009.250.253.

Mullan, D.J., Reynolds, M.P., 2010. Quantifying genetic effects of ground cover on soil water evaporation using digital imaging. Funct. Plant Biol. 37, 703–712. https://doi.org/10.1071/FP09277.

Nguyen, G.N., Norton, S.L., Rosewarne, G.M., James, L.E., Slater, A.T., 2018. Automated phenotyping for early vigour of field pea seedlings in controlled environment by colour imaging technology. PLoS One 13 (11), e0207788. https://doi.org/10.1371/journal.pone.0207788.

Nuttall, J.G., Perry, E.M., Delahunty, A.J., O'Leary, G.J., Barlow, K.M., Wallace, A.J., 2019. Frost response in wheat and early detection using proximal sensors. J. Agro Crop Sci. 2019 (205), 220–234. https://doi.org/10.1111/jac.12319.

Pandey, B.R., Burton, W., Salisbury, Nicolas, M.E., 2016. Non-destructive measurement of canopy cover is an alternative to biomass sampling at anthesis to predict yield of canola-quality Brassica juncea. Aus 10 (4), 482–489. https://doi.org/10.21475/ajcs.2016.10.04.p7103x.

Potgieter, A.B., George-Jaeggli, B., Chapman, S.C., Laws, K., Suárez Cadavid, L.A., Wixted, J., Watson, J., Eldridge, M., Jordan, D.R., Hammer, G.L., 2017. Multispectral imaging from an unmanned aerial vehicle enables the assessment of seasonal leaf area dynamics of sorghum breeding lines. Front. Plant Sci. 8, 1532. https://doi.org/10.3389/fpls.2017.01532.

Pix4D, 2017. Pix4Dmapper 4.1 User Manual. Pix4D SA, Lausanne, Switzerland.

Rebetzke, G.J., Richards, R.A., 1999. Genetic improvement of early vigour in wheat. Aust. J. Agric. Res. 50 (3), 291–302. https://doi.org/10.1071/A98125.

Rebolledo, M.C., Dingkuhn, M., Péré, P., McNally, K.L., Luquet, D., 2012. Developmental dynamics and early growth vigour in rice. I. Relationship between development rate (1/phyllochron) and growth. J. Agron. Crop Sci. 198 (5), 374–384. https://doi.org/10.1111/j.1439-037X.2012.00528.x.

Sadras, V.O., Lake, L., Chenu, K., McMurray, L.S., Leonforte, A., 2012. Water and thermal regimes for field pea in Australia and their implications for breeding. Crop Pasture Sci. 63, 33–44. https://doi.org/10.1071/CP11321.

Stamatis, I.S., Taskos, D., Tsadila, E., Christofides, C., Tsadilas, Christos, C.D., Schepers, J.S., 2009. Comparison of passive and active canopy sensors for the estimation of vine biomass production. Percision Agric. 11 (3), 306–315. https://doi.org/10.1007/s11119-009-9131-3.

Su, J., Liu, C., Coombes, M., Hu, X., Wang, C., Xu, X., Li, Q., Guo, L., Chen, W.H., 2018. Wheat yellow rust monitoring by learning from multispectral UAV aerial imagery. Comput. Electron. Agric. 155, 157–166. https://doi.org/10.1016/j.compag.2018.10.017.

Sultana, S.R., Ali, A., Ahmad, A., Mubeen, M., Zia-Ul-Haq, M., Ahmad, S., Ercisli, S., Jaafar, H.Z.E., 2014. Normalized Difference Vegetation Index as a Tool for Wheat Yield Estimation: A case Study from Faisalabad. Pak. Sci. World J. 2014, 1–8. https://doi.org/10.1155/2014/725326.

Tan, C., Zhang, P., Zhou, X., et al., 2020. Quantitative monitoring of leaf area index in wheat of different plant types by integrating NDVI and Beer-Lambert law. Sci. Rep. 10, 929. https://doi.org/10.1038/s41598-020-57750-z.

Turner, N.C., Nicolas, M.E., 1998. Early vigour: a yield-positive characteristic for wheat in drought-prone Mediterranean-type environments. In: Behl, R.K., Singh, D.P., Lodhi, G.P. (Eds.), Crop Improvement for Stress Tolerance. CCSHAU, Hisar and MMB, New Delhi, pp. 47–62.

Ullah, S., Bramley, H., Mahmood, T., Trethowan, R., 2019. A strategy of ideotype development for heat-tolerant wheat. J. Agron. Crop. Sci. 206 (2), 229–241. https://doi.org/10.1111/jac.12378.

VSN International, 2015. Genstat for Windows, twentyth ed. VSN International, Hemel Hempstead, UK (Web page: Genstat.co.uk).

Zhou, Y., Zhu, H.Z., Cai, S.B., He, Z.H., Zhang, X.K., Xia, X.C., Zhang, G.S., 2007. Genetic improvement of grain yield and associated traits in the southern China winter wheat region: 1949 to 2000. Euphytica 157, 465–473. https://doi.org/10.1007/s10681-007-9376-8.

Ward, P.R., Hall, D.J.M., Micin, S.F., Whisson, K., Willis, T.M., Treble, K., Tennant, D., 2007. Water use by annual crops. 1. Role of dry matter production. Crop Pasture Sci. 58, 1159–1166. https://doi.org/10.1071/AR07076.

Winterhalter, L., Mistele, B., Schmidhalter, U., 2012. Assessing the vertical foot-print of reflectance measurements to characterize nitrogen uptake and biomass distribution in maize canopies. Field Crops Res. 129, 144–229. https://doi.org/10.1016/j.fcr.2012.01.007.

Winterhalter, L., Mistele, Urs Schmidhalter, U., 2013. Evaluation of active and passive sensor systems in the field to phenotype maize hybrid with high throughput. Field Crops Res. 154, 236–245. https://doi.org/10.1016/j.fcr.2013.09.006.

Xue, J., Su, B., 2017. Significant remote sensing vegetation indices: a review of developments and applications. J. Sens., 17 https://doi.org/10.1155/2017/1353691 vol. 2017.